Asian Journal of Chemistry; Vol. 34, No. 6 (2022), 1513-1516

ASIAN JOURNAL OF CHEMISTRY

https://doi.org/10.14233/ajchem.2022.23518


# Isolation of Nanocellulose from Aquatic Wetland Plant-*Eleocharis dulcis*

S. SUNARDI[1,2,*], W.T. ISTIKOWATI[2,3], D.I. SARI[4], D.H.Y. YANTO[5] and A. KAMARI[6]

[1]Department of Chemistry, Faculty of Mathematics and Natural Science, Lambung Mangkurat University, Banjarbaru 70714, Indonesia
[2]Wetland-Based Materials Research Center, Lambung Mangkurat University, Banjarbaru 70714, Indonesia
[3]Faculty of Forestry, Lambung Mangkurat University, Banjarbaru 70714, Indonesia
[4]Pharmacy Department, Faculty of Mathematics and Natural Science, Lambung Mangkurat University, Banjarbaru 70714, Indonesia
[5]Research Center for Applied Microbiology, National Research and Innovation Agency, Indonesia
[6]Department of Chemistry, Faculty of Science and Mathematics, Universiti Pendidikan Sultan Idris, 35900, Tanjung Malim, Perak, Malaysia

*Corresponding author: E-mail: sunardi@ulm.ac.id

*Received*: 6 September 2021; *Accepted*: 13 March 2022; *Published online*: 18 May 2022; AJC-20815

*Eleocharis dulcis* is a sustainable wetland material available in enormous quantities in Kalimantan, Indonesia. This study aimed to evaluate the suitability of the acid hydrolysis method for the isolation of nanocellulose of *E. dulcis*. The isolation process started with delignification, followed by the removal of hemicellulose to produce cellulose. The hydrolysis was performed at 45 ºC for 60 and 120 min, respectively, using sulphuric acid. Furthermore the nanocellulose was characterized using particle size analyzer, Fourier transform infrared spectroscopy and X-ray diffractions. The particle size analysis showed that the diameter of the nanocellulose was affected by hydrolysis time. In addition, the X-ray diffractions results showed that the crystallinity index of the nanocellulose was 71.99% and 71.61% for the acid hydrolysis time of 60 min and 120 min, respectively. This study also demonstrated that the aquatic wetland plant, *E. dulcis* has a good potential for nanocellulose production in Indonesia.

**Keywords: *Eleoharis dulcis*, Nanocellulose, Wetland plant, Acid hydrolysis.**

## INTRODUCTION

Nanocellulose or cellulose nanoparticle is cellulose with a diameter less than 100 nm and characterized by a high modulus, surface area, and crystalline character. In recent years, there is a growing interest in producing nanocellulose from numerous sources, especially from plants, such as bagasse [1], sisal fiber [2], residue of banana [3], wood and plantation waste [4].

The extraction of nanocellulose with the acid hydrolysis has been widely studied using various cellulose sources [4,5]. Furthermore, hydrochloric acid, phosphoric acid and sulphuric acid have been regarded as the most common and effective acids to remove the amorphous portion in the isolation process of nanocellulose, sparing the crystalline part of cellulose in a colloidal suspension [6]. Sulphuric acid can produce a negative surface of the nanocellulose and increase the suspen-sion stability due to electrostatic repulsion [7]. The cellulose nano-particles have a high surface area, stiffness and crystall-inity, appropriate for applications in composites for food packa-ging as filler or reinforcing agent [8] and biomedical applications.

*Eleocharis dulcis* is an aquatic plant that can adapt and grow well in acid sulfate-rich soils or swamps. In Indonesia, their stems are used to make various handicrafts such as mats, bags, and others and as animal feed. Furthermore, *E. dulcis* is cheap and abundant in the wetland region in Kalimantan, Indonesia and consists of more than 40% of cellulose [9,10]. Although many researches demonstrated the production of nanocellulose from various resources, there is no information on the isolation of *E. dulcis* nanocellulose. The study aimed to produce and characterize nanocelluloses from *E. dulcis* by acid hydrolysis using sulfuric acid at a mild temperature. In addition, investigation was carried out on the effect of the period of acid hydrolysis treatment on the particle size and crystallinity of the nanocelluloses.

## EXPERIMENTAL

Samples preparation: *E. dulcis* was harvested from South Kalimantan in Indonesia. The stems were washed, cut, dried, and ground. The powder was further sieved through a 60 mesh and stored in a plastic container at room temperature.

**Isolation of α-cellulose:** Extraction of air-dried *E. dulcis* powder (5 g) was done with 240 mL mixture of ethanol and toluene (1:2, v/v) for 6 h using a Soxhlet extractor and then kept at room temperature for a day to remove the residual solvents. The free extracted sample (2.5 g) was delignified with 150 mL of distilled water in an Erlenmeyer flask. Furthermore, 1 g of $NaClO_2$ and 0.2 g of $CH_3COOH$ were added to the flask and heated at 70 ºC in a water bath. After this process, the sample was then clarified and rinsed with distilled water and acetone. The sample was soaked in 17.5% m/v NaOH for 4 min and then homogenized by a glass stick for 5 min. Distilled water (25 mL) was added after 5 min to the suspension, allowed to stand for 5 min and further refiltered by using a glass filter to isolate cellulose from holocellulose.

**Isolation of nanocellulose:** Approximately 5 g of *E. dulcis* cellulose was added to 100 mL of $H_2SO_4$ (50% (v/v)) at 45 ºC and agitated at 1.200 rpm for 60 min and 120 min, respectively. Distilled water (500 mL) was then added to discontinue the reaction. The suspension was centrifuged for 30 min, and the filtrate was discarded. Furthermore, the nanocellulose suspension was dialyzed using a dialysis membrane (12,000-14m000 MWCO) with water until the neutral pH of suspension was attained. The nanocellulose suspension was sonicated by using an ultrasonic bath for 5 min and the sample was then kept in a refrigerator at 5-7 ºC. In addition, the sample was mixed with chloroform to avoid any bacterial growth until when required.

**FTIR analysis:** FTIR analysis of the cellulose and nanocellulose samples was carried out using an attenuated total reflectance-infrared (ATR-IR) spectrophotometer (ALPHA-P model, Bruker Optics, Germany) and scanned at a range of 4000-400 $cm^{-1}$. Furthermore, based on the literature, the typical band spectra of the cellulose and nanocellulose were recognized.

**XRD analysis:** X-ray diffraction of nanocellulose samples were analyzed using a diffractometer Shimadzu XRD-7000, which operated at room temperature within a 2θ range from 5 to 40º and a scan rate of 1º $min^{-1}$, with a current of 30 mA and Cu*K*α radiation at a power of 40 kV. The cellulose index of crystallinity (CrI) was evaluated using Segal's equation [11].

$$CrI = \left( \frac{I_{002} - I_{am}}{I_{002}} \right) \times 100 \quad (1)$$

where $I_{002}$ is the maximum peak intensity of the 0 0 2 lattice diffraction at 2θ = 21.9º, and $I_{am}$ is the minimum intensity between the 0 0 2 and 0 1 1 lattice diffraction. $I_{002}$ corresponds to the crystalline part of nanocellulose and Iam correspond to the amorphous region of nanocellulose. The X-ray diffraction patterns of cellulose crystallites estimated their average thickness by using Scherrer's equation [12]:

$$D_{hkl} = \frac{K\lambda}{\beta_{1/2} \cos\theta} \quad (2)$$

where $D_{hkl}$ is the crystallite size of cellulose, K is the Scherrer constant, λ is the wavelength of X-ray, θ is the Bragg angle and $\beta_{1/2}$ is the half-height width at maximum intensity of the diffraction band.

**Particle size analyzer:** The particle size distribution of nanocellulose was evaluated using a particle size analyzer called Malvern Zetasizer Nano. Measurement of particle size utilizes the principle of visible light scattering. Therefore, the diluted suspension of the nanocellulose was placed in the cuvette and passed through the visible light that diffraction occurred.

## RESULTS AND DISCUSSION

Fig. 1 shows the photograph of visual appearance of the stable aqueous suspension of nanocrystalline cellulose, produced from *E. dulcis* by 50% $H_2SO_4$ at 45 ºC for 60 min (**1**) and 120 min (**2**). The suspensions were white, milky, turbid and stable for a long time. These photograps confirmed the hydrolysis treatment by sulfuric acid has formed sulfate groups which yield a negative surface charge on nanocelluloses surfaces. Furthermore, these negative sulfate charges will produce an electrostatic repulsion between the nanocellulose particles and avoid aggregation. The stable suspension of nanocrystalline cellulose presents a piece of principal evidence about the hydrolysis of cellulose, it is an indicator of the presence of nanoparticles.


Fig. 1. Aqueous suspension of *E. dulcis* nanocellulose (1) hydrolysis for 60 min and (2) 120 min

**FTIR studies:** FTIR spectroscopy was used to assess the chemical composition changes due to acid hydrolysis process on *E. dulcis* cellulose (Fig. 2). Furthermore, two dominant transmittance peaks in the FTIR spectra of cellulose and nanocellulose were detected in the region at 3400-2900 $cm^{-1}$ and 1700-800 $cm^{-1}$, respectively. Generally, nanocellulose samples produced with different period of time of hydrolysis demonstrate a similar FTIR spectrum. Based on the FTIR spectra in Fig. 2, there was no significant change in the cellulose structure and chemical components because of the sulfuric acid hydrolysis process for 60 and 120 min, respectively. In addition, a main and broad transmittance band located at peak in the region about 3330 $cm^{-1}$ and 2890 $cm^{-1}$, respectively, are recognized to O-H groups stretching in cellulose and contributed to stretching vibration of the aliphatic saturated C-H in cellulose [9,13].

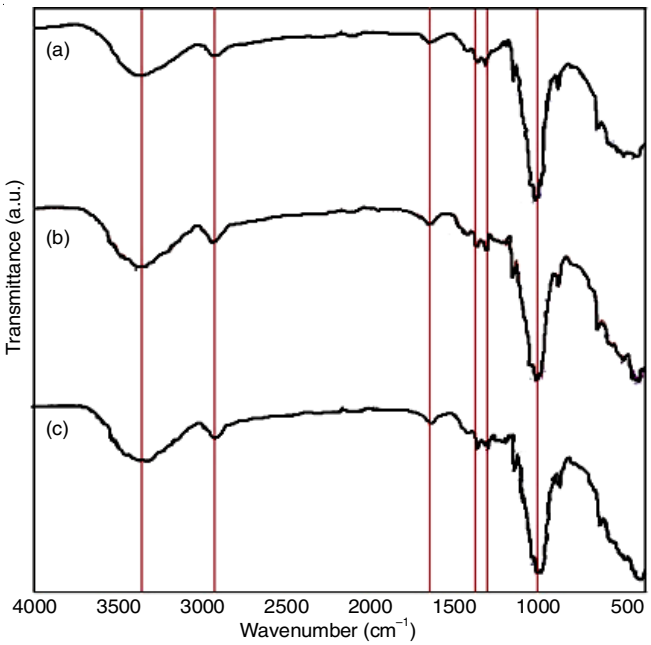


Fig. 2. FTIR spectra of *E. dulcis* cellulose (a) and nanocellulose (b) hydrolysis for 60 min (c) 120 min

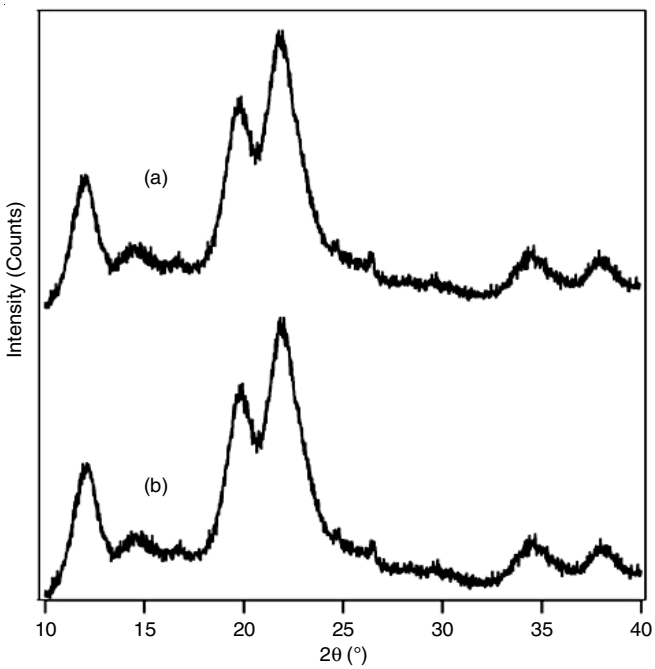


Fig. 3. XRD diffractogram of *E. dulcis* nanocellulose (a) hydrolysis for 60 min and (b) 120 min

A band detected at around 1640 $cm^{-1}$ in the FTIR spectra of cellulose and nanocellulose was recognized by the bending of O-H from the adsorbed water because of the interaction between water and cellulose/nanocellulose. Meanwhile, the vibration peak detected at around 1366 $cm^{-1}$ in cellulose and nanocelluloses from *E. dulcis* samples corresponded to C-O, and C-H bending vibration in the aromatic rings of polysaccharide. A transmittance band at around 1023 $cm^{-1}$ is associated with the stretching of C-O and rocking vibration of C-H in the pyranose ring [14]. In addition, the band at 894 $cm^{-1}$ referred to the β 1-4 gycosidic bond between the glucose monomer in the cellulose [15]. The existence of this peak in the nanocellulose spectra is fascinating because this peak indicates that the cellulosic part is remain through the hydrolysis process.

**XRD studies:** Fig. 3 shows the X-ray diffractogram of nanocellulose obtained under different hydrolysis time and the crystallinity values, respectively. Furthermore, the X-ray diffraction patterns of nanocellulose at 60 min and at 120 min are the characteristic of cellulose polymorphs. The typical cellulose I and cellulose II structures were observed in the diffraction patterns for each nanocellulose. Cellulose I has strong crystalline peaks at 2θ 14.5º and 22º corresponding to the (110) and (002) planes of crystals and weak crystalline peaks at 2θ 34.8º to the (004) plane. Meanwhile, the peak at 2θ 12.1º and 19.8º corresponds to cellulose II structure [16]. Probably, the existence of cellulose II is related to the agglomeration of nanocellulose after drying procedure [17]. Consequently, the intensity of X-ray diffraction peaks of nanocellulose at around 2θ 14.5º and 22º slightly increase from 60 min to 120 min hydrolysis time, which indicated the removal of amorphous part of cellulose.

The value of crystallinity index (CrI), interplanar distance (*d*-spacing) and crystal size of nanocrystalline cellulose calculated using eqn. 2. The three main crystals size (L) and interplanar distance (*d*-spacing) of nanocrystalline cellulose for each crystal plane (110), (110) and (200) are represented with the symbols $L_1$, $L_2$, $L_3$ and $d_1$, $d_2$, $d_3$, respectively (Table-1). Therefore, the values of interplanar distance of nanocrystalline cellulose are essential due to these values and can provide modifications in the form of nanocrystalline cellulose structure (Iα and Iβ). The crystal size (L) reveals the nanocrystalline cellulose stiffness [18]. Additionally, the *d*-spacing values of nanocrystalline cellulose did not change drastically because of the hydrolysis process of *E. dulcis*. However, the crystallite sizes were more sensitive to the hydrolysis process and changed significantly.

The CrI value of the nanocrystalline cellulose with different hydrolysis times (60 and 120 min) calculated using eqn. 1 gave values of 71.99% and 71.61%, respectively and were not statistically different. Consequently, the slight decrease in crystallinity of nanocrystalline cellulose with 120 min of hydrolysis time indicated that the acid hydrolysis process eliminated the amorphous part and attacked the crystalline part of cellulose. The comparable data of the influence of hydrolysis time on nanocrystalline cellulose isolation was reported by Chen *et al*. [19].

TABLE-1
CRYSTALLINITY PARAMETER OF NANOCELLULOSE FROM *E. dulcis* UNDER DIFFERENT HYDROLYSIS TIME

| Sample | d-spacing (nm) | | | Crystallite (nm) | | | CrI (%) |
|---|---|---|---|---|---|---|---|
| | $d_1$ | $d_2$ | $d_3$ | $L_1$ | $L_2$ | $L_3$ | |
| Nanocellulose 60 | 0.611 | 0.533 | 0.405 | 6.2 | 14.1 | 4.1 | 71.99 |
| Nanocellulose 120 | 0.611 | 0.532 | 0.401 | – | – | 64.8 | 71.61 |

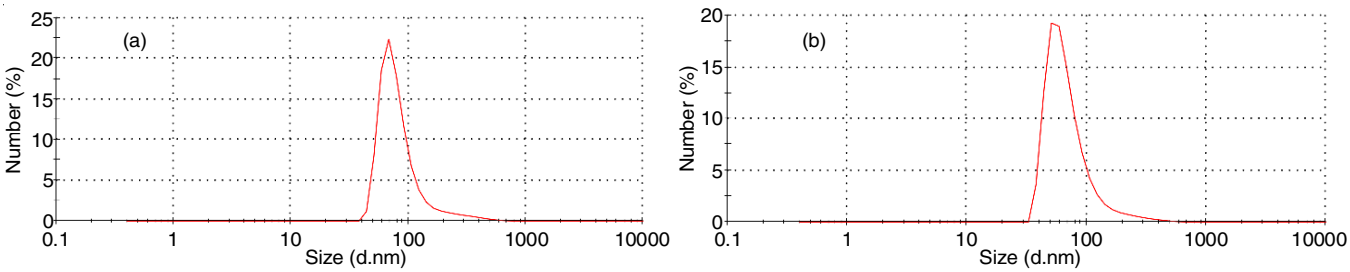


Fig. 4. Particle size distribution by number of *E. dulcis* nanocellulose (a) hydrolysis for 60 min and (b) 120 min

Dynamic Light Scattering (DLS) is a popular method to analyze the particle size distribution of nanoparticles in emulsions or suspensions. Nevertheless, it is principal to underline that DLS methods assume that all of the particles are in the same shape (spherical) and the particle size relies on the particle direction in suspension [20]. Generally, the geometrical dimension for nanocellulose includes the width in tenths of nanometers and the length in hundredths of nanometers. In this research, the width of nanocelluloses from *E. dulcis* under 100 nm were successfully produced (Fig. 4). According to the results, an increase in the acid hydrolysis time decreases the nanocellulose size, including the *z*-average (particle size distribution) from 336.5 nm to 256.3 nm. Furthermore, it was observed that the diameter ranges from 36.17 nm to 169.8 nm at 60 min of hydrolysis time (Fig. 4). It showed homogeneity at 71.51 nm in diameter due to the longer hydrolysis process. Therefore, these results showed that acid hydrolysis for 120 min was the best treatment to produce nanocellulose in homogeneity diameter.

## Conclusion

In this study, nanocrystalline cellulose was successfully extracted from the *Eleocharis dulcis* by acid hydrolysis process for the first time. Furthermore, this process resulted in the production of a stable suspension because of the negatively charged sulfate group. Using the acid hydrolysis method, the nanocellulose had a CrI value about 72% and a diameter in the range of 36.17 nm to 169.8 nm. Subsequently, a diameter of 71.51 nm for 60 min and 120 min hydrolysis time, respectively. This study demonstrates the potential of *E. dulcis* biomass as a suitable raw material for the production of nanocellulose.

## ACKNOWLEDGEMENTS

The authors thank Biomaterials Chemistry Laboratory Lambung Mangkurat University for the laboratory facilities and Ministry of Education, Culture, Research and Technology of Republic Indonesia for the financial support of Research Grant 2021 (Contract number 119/E.4.1/AK.04.PT/2021).

## CONFLICT OF INTEREST

The authors declare that there is no conflict of interests regarding the publication of this article.

## REFERENCES

1. E.M. Teixeira, T.J. Bondancia, K.B.R. Teodoro, A.C. Corrêa, J.M. Marconcini and L.H.C. Mattoso, *Ind. Crops Prod.*, **33**, 63 (2011); https://doi.org/10.1016/j.indcrop.2010.08.009
2. J.I. Morán, V.A. Alvarez, V.P. Cyras and A. Vázquez, *Cellulose*, **15**, 149 (2008); https://doi.org/10.1007/s10570-007-9145-9
3. R. Zuluaga, J.L. Putaux, A. Restrepo, I. Mondragon and P. Ganán, *Cellulose*, **14**, 585 (2007); https://doi.org/10.1007/s10570-007-9118-z
4. M. Jonoobi, A. Khazaeian, P.M. Tahir, S.S. Azry and K. Oksman, *Cellulose*, **18**, 1085 (2011); https://doi.org/10.1007/s10570-011-9546-7
5. E. Qua, P. Hornsby, H. Sharma and G. Lyons, *J. Mater. Sci.*, **46**, 6029 (2011); https://doi.org/10.1007/s10853-011-5565-x
6. R.J. Moon, A. Martini, J. Nairn, J. Simonsen and J. Youngblood, *Chem. Soc. Rev.*, **40**, 3941 (2011); https://doi.org/10.1039/c0cs00108b
7. M.M. de Souza Lima and R. Borsali, *Macromol. Rapid Commun.*, **25**, 771 (2004); https://doi.org/10.1002/marc.200300268
8. D.J. Gardner, G.S. Oporto, R. Mills and M.A.S.A. Samir, *J. Adhes. Sci. Technol.*, **22**, 545 (2008); https://doi.org/10.1163/156856108X295509
9. N.M. Sunardi, N.M. Febriani and A.B. Junaidi, *AIP Conf. Proc.*, **1868**, 020008 (2017); https://doi.org/10.1063/1.4995094
10. Sunardi, W.T. Istikowati and D.I. Sari, *J. Phys. Conf. Ser.*, **1397**, 012031 (2019); https://doi.org/10.1088/1742-6596/1397/1/012031
11. L. Segal, J. Creely, A. Martin Jr. and C. Conrad, *Text. Res. J.*, **29**, 786 (1959); https://doi.org/10.1177/004051755902901003
12. H.P. Klug and L.E. Alexander, X-Ray Diffraction Procedures: For Polycrystalline and Amorphous Materials, 2nd Edition, by pp 992 Wiley-VCH, Ed. 2, pp. 992 (1974).
13. S. Sunardi, W.T. Istikowati, F. Ishiguri and S. Yokota, *AIP Conf. Proc.*, **2026**, 020024 (2018); https://doi.org/10.1063/1.5064984
14. H. Kargarzadeh, R. M. Sheltami, I. Ahmad, I. Abdullah and A. Dufresne, *Polymer*, **56**, 346 (2015); https://doi.org/10.1016/j.polymer.2014.11.054
15. A. Mandal and D. Chakrabarty, *Carbohydr. Polym.*, **86**, 1291 (2011); https://doi.org/10.1016/j.carbpol.2011.06.030
16. M. Ago, T. Endo and T. Hirotsu, *Cellulose*, **11**, 163 (2004); https://doi.org/10.1023/B:CELL.0000025423.32330.fa
17. W.P. Flauzino Neto, H.A. Silvério, N.O. Dantas and D. Pasquini, *Ind. Crops Prod.*, **42**, 480 (2013); https://doi.org/10.1016/j.indcrop.2012.06.041
18. K.C.C.C. Benini, H.J.C. Voorwald, M.O.H. Cioffi, M.C. Rezende and V. Arantes, *Carbohydr. Polym.*, **192**, 337 (2018); https://doi.org/10.1016/j.carbpol.2018.03.055
19. Y. Chen, C. Liu, P.R. Chang, X. Cao and D.P. Anderson, *Carbohydr. Polym.*, **76**, 607 (2009); https://doi.org/10.1016/j.carbpol.2008.11.030
20. A.N. Frone, D.M. Panaitescu, D. Donescu, C.I. Spataru, C. Radovici, R. Trusca and R. Somoghi, *BioResources*, **6**, 487 (2010); https://doi.org/10.15376/biores.6.1.487-512